

MAPPING LAND COVER TIME SERIES USING LANDSAT-8 AND SENTINEL-1 IN SOUTH KALIMANTAN

I. L. Sari^{1,2}, C. J. Weston¹, G. J. Newnham³, L. Volkova¹

¹ School of Ecosystem and Forest Sciences, Faculty of Science, The University of Melbourne, Creswick, Australia -
Weston@unimelb.edu.au, Lubav@unimelb.edu.au

² Research Center for Remote Sensing, National Research and Innovation Agency (BRIN), Jakarta, Indonesia -
inggit.lolita.sari@brin.go.id

³ CSIRO Land and Water, Clayton South, Australia - Glenn.Newnham@csiro.au

Commission IV, WG 7

KEY WORDS: Bayesian, Time Series, Land Cover, Classification, Kalimantan.

ABSTRACT:

Remote sensing has been widely used for forest monitoring. However, most forest monitoring systems largely rely on optical images that limit temporal analyses due to cloud cover, particularly in the tropics. The current study used integration of optical Landsat-8 and Sentinel-1 SAR to produce individual year land cover classification maps for Kalimantan, Indonesia that differentiate between native forest and tree plantations, such as oil palm and rubber. We applied a Bayesian network to produce a time series of land cover classification that improved accuracy of individual year land cover maps. Accuracy assessment using a confusion matrix showed that final map had overall accuracy of 90%, while user's and producer's accuracy for each land cover class was above 85%, except non-forest, which had 76% producer's accuracy due to errors in the classification between young rubber plantations and non-forest. Improved maps will support Indonesia's national forest monitoring system and sustainable forest management.

1. INTRODUCTION

Major deforestation in the tropics is driven by agricultural expansion, including timber logging (Hosonuma et al., 2012). Borneo island has experienced vast and rapid deforestation, with forest loss of around 6.04 M ha between 2000–2017 (Gaveau et al., 2018). Around 51% of this forest loss was for plantation expansion, such as oil palm and rubber plantations (Gaveau et al., 2018).

Remote sensing has been used for several decades to monitor forest extent and change, drawing on optical images such as those from the Landsat series of satellites (Romijn et al., 2015; Sari et al., 2021a). However, intense cloud cover limits the ability of optical images to detect temporal changes in vegetation cover and types in tropical countries (Massey et al., 2018; Sari et al., 2021a).

Synthetic Aperture Radar (SAR) systems, such as ALOS PALSAR, and Sentinel-1 offer the ability to penetrate clouds, smoke, and haze (Hoekman, Vissers, and Wielaard, 2010; Motohka et al., 2014). Furthermore, SAR data is sensitive to vegetation structure, moisture content, and ground conditions (Pohl, 2014; Miettinen, Liew, and Kwoh, 2015).

Improvement of forest monitoring may be possible by combining optical and SAR satellite sensors to reduce limitations imposed by persistent cloud cover. Integration of optical and SAR images has already been shown to improve forest classification accuracy (Sarzynski et al., 2020; Sari et al., 2022). However, employing multitemporal constraints on classification may help to further reduce the uncertainty in the land cover classification (Ban, 2016; LAPAN, 2014).

We showed that integration of Landsat-8 optical images and Sentinel-1 SAR images using a decision tree could be used to

improve the classification accuracy of native forests, oil palm and rubber plantations, and non-forest areas in South Kalimantan province (Sari et al., 2022). This paper describes the use of a Bayesian network for time series classification to further refine individual year land cover maps from 2015 to 2017. The development of these improved time series of land cover maps aims to support Indonesia's national forest monitoring program, and sustainable forest management.

2. MATERIALS AND METHODS

2.1 Study Area

The study area is situated in the north part of South Kalimantan province, Indonesia, covering 62,500 hectares (Figure 1). Native forests, oil palm plantations, rubber plantations, and non-forest such as settlements, paddy fields, shrubs, and grasslands exist in the region. The extent of oil palm and rubber plantations increased in this province by 42.5% over the past seventeen years, from 294,982.72 hectares in 2000 to 693,619 hectares in 2017 (BPS-Statistics Indonesia, 2000; BPS-Statistics Indonesia, 2018).

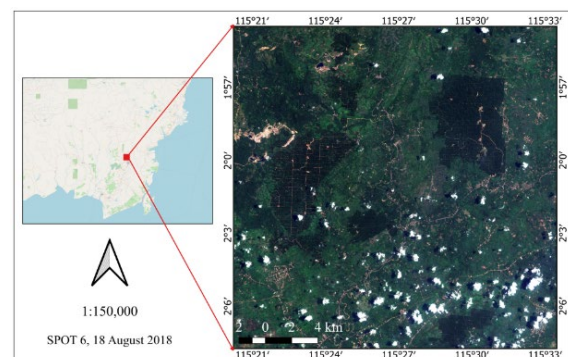


Figure 1. Study area in South Kalimantan province.

2.2 Satellite image pre-processing

A time series of Landsat-8 optical and Sentinel-1 SAR images, from 2015 to 2017, were mosaiced at 25 m resolution and used as the main data to produce individual year land cover map, using the decision tree approach described by Sari et al. (2022).

Landsat-8 images with less than 50% cloud cover were downloaded from the USGS Earth Resources Observation and Science (EROS) Center (2019). Sentinel-1A Interferometric Wide (IW) swath mode Level-1 Ground Range Detected (GRD) images for each individual year were downloaded from the Alaska Satellite Facility Distributed Active Archive Center (2019).

The Landsat-8 images pre-processing method is outlined in previous publications (LAPAN, 2014; Sari et al., 2022). The image pre-processing consists of scene selection, geometric, radiometric, terrain correction, cloud masking, and mosaicking. The annual mosaics of Landsat-8 images consist of six multi-spectral image bands of blue, green, red, near infrared, short-wave infrared 1, and short-wave infrared 2, and processed top of atmosphere (TOA) and bidirectional reflectance distribution function (BRDF) correction.

The Sentinel-1 images pre-processing consists of applying an update of precise orbit acquisition information, radio-metric calibration, and terrain correction to remove terrain effects. The mosaic Sentinel-1A images with dual-polarization of VV + VH bands were used in this study to analyse the backscatter intensity of the land cover classes.

2.3 Bayesian time series classification

Bayesian networks use prior information of land cover to predict and track past land cover changes (Lee, Cardille, and Coe, 2020). A Bayesian network was used to improve time series classification and update the certainty of land cover based on prior land cover information and plantation occurrence images. The prior land cover was the individual land cover classifications to integrate Landsat-8 and Sentinel-1 to produce four land cover classes described in Section 2.4. The plantation occurrence images for improvement of oil palm and rubber discrimination are described in Section 2.5. Thus, the steps to utilise a Bayesian network for temporal processing of these inputs were as follows:

- Create a land cover change probability matrix using individual land cover classifications from 2015 to 2017. That is, for these two years, changes in the four classes were analysed and allocated to one of 16 land cover change categories.
 - Create oil palm and rubber plantation occurrence probability maps for 2015 to 2017 (see Section 2.5).
- Calculate the probability of land cover classes for the preceding year based on information from the following map for native forest and non-forest classes, using the Bayesian equation (Eq.1):

$$P(\text{Map}_{2016}|\text{Map}_{2017}) = \frac{P(\text{Map}_{2017}|\text{Map}_{2016})P(\text{Map}_{2016})}{P(\text{Map}_{2017})}, \quad (1)$$

- Calculate the probability of land cover classes in 2016 for the rubber plantation class based on the 2017 map using the equation (Eq.2):

$$P(\text{Map}_{2016}|\text{Map}_{2017}, \text{Rubber}_{2016}) =$$

$$\frac{P(\text{Map}_{2017}, \text{Rubber}_{2016}|\text{Map}_{2016})P(\text{Map}_{2016})}{P(\text{Map}_{2017}, \text{Rubber}_{2016})}, \quad (2)$$

Land cover probability of a transition to the oil palm class was calculated based on the probability of the occurrence of oil palm (i.e., substituting rubber with oil palm in Eq. 2).

- The decision if a transition should occur was based on the following rule: if the probability for stable class (similar to previous) is greater than the probability for change class then the decision will be stable (similar to previous class), and if the probability for change class is greater than the stable class then the decision class will change to a new class.
- Validate the oil palm and rubber plantation classes using the plantation occurrence boundary to reduce speckle class due to the pixel-based method (see Section 2.5).
- Apply the same Bayesian network processing in the forward time series direction to produce a final land cover map.

2.4 Individual year land cover classification

The individual year land cover classification was developed from the annual forest and non-forest maps combined with oil palm and rubber plantation algorithms developed from Landsat-8 and Sentinel-1 (LAPAN, 2014; Sari et al., 2022). The individual year land cover classification method has been outlined in Sari et al. (2022).

2.5 Plantation occurrence images

The oil palm and rubber plantations occurrence were used as additional information for assessing the plantation occurrence. The oil palm and rubber occurrence maps were created using a combination between NDVI and SWIR 1 for oil palm occurrence, and NDMI and SWIR 1 for rubber occurrence. The thresholds in the decision tree were determined from the histogram of values for training samples of oil palm and rubber. The boundary for the oil palm and rubber plantations were produced from the mosaic of the nearest year plantation occurrence image with a median filter applied.

2.6 Accuracy assessment of land cover map

A confusion matrix was used to measure the accuracy of the 2017 classification maps, including overall accuracy, producer's accuracy, and user's accuracy. The map accuracy assessment was based on stratified random sampling with 196 validation points (Sari et al., 2021b). One scene of high-resolution SPOT 6 images (resolution 1.5 m) acquired on 18 August 2018 was used as the reference images with validation based on a minimum area of 50 x 50 m for each of 196 points.

3. RESULTS AND DISCUSSION

The mosaic images of Landsat-8 and Sentinel-1 to develop individual land cover classification from 2015–2017 are shown in Figure 2. These Landsat-8 images are depicted in a composite of short-wave infrared 1, near infrared, and red band. While Sentinel-1 images in Figure 2 are depicted in composites of the Grey Level Co-occurrence Matrix (GLCM) variance texture of VH-VV. Samples for decision-making using Bayesian network to produce time series classification maps for 2016 and 2017 are described in Table 1–Table 4.

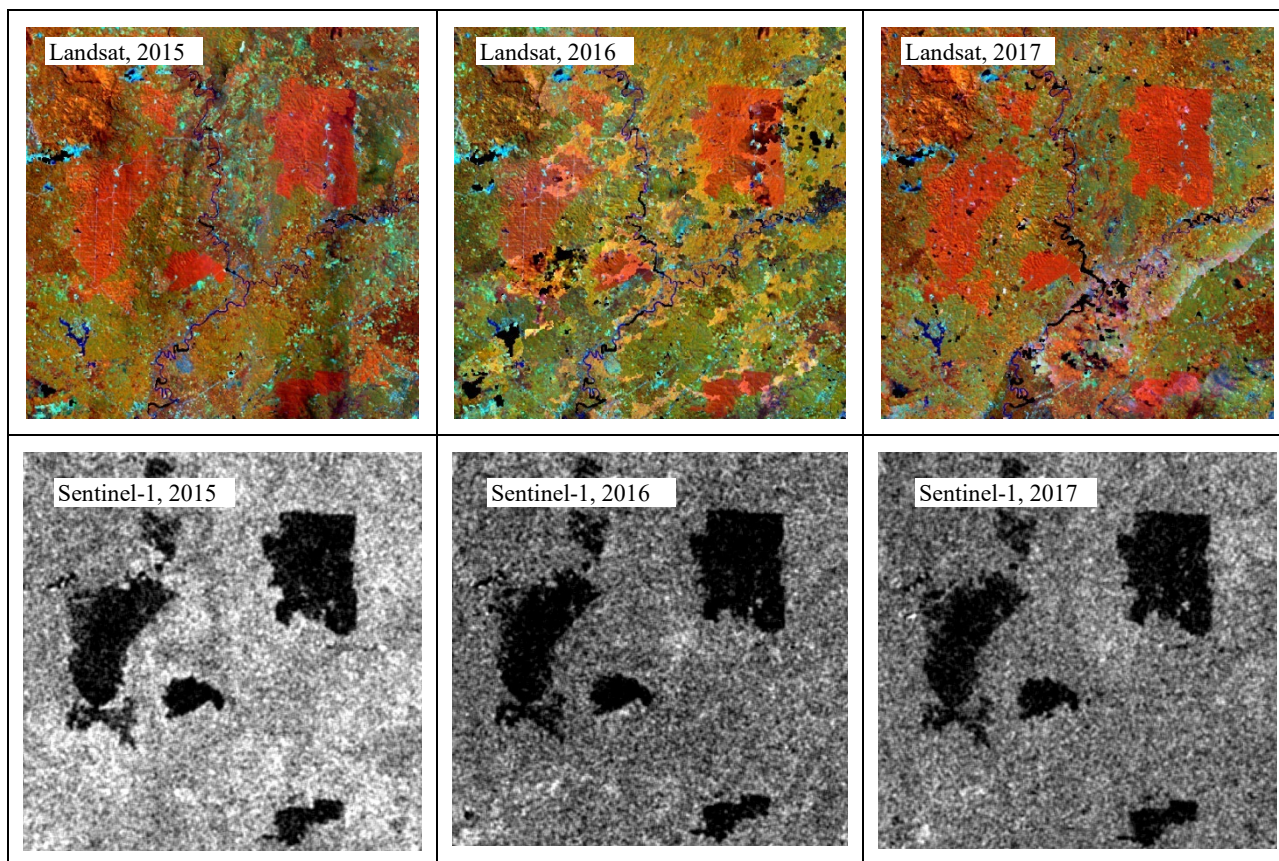


Figure 2. Mosaic images of Landsat-8 and Sentinel-1 from 2015–2017.

2016 \ 2017	Land cover class				
	Native forest	Oil palm	Rubber	Non-forest	Total
Native forest	0.223	0.010	0.013	0.008	0.254
Oil palm	0.009	0.110	0.004	0.003	0.126
Rubber	0.009	0.002	0.213	0.101	0.325
Non-forest	0.004	0.003	0.122	0.166	0.295
Total	0.244	0.125	0.353	0.278	1.000

Table 1. Land cover changes map probability for 2016–2017.

2016 \ 2017	Land cover class		
	Rubber	Non-rubber	Total
Native forest	0.025	0.229	0.254
Oil palm	0.002	0.124	0.126
Rubber	0.200	0.125	0.325
Non-forest	0.070	0.224	0.295
Total	0.297	0.703	1.000

Table 2. Rubber occurrence probability in 2016.

2016 \ 2017	Land cover class		
	Oil palm	Non-oil palm	Total
Native forest	0.241	0.013	0.254
Oil palm	0.117	0.009	0.126
Rubber	0.314	0.012	0.325
Non-forest	0.190	0.104	0.295
Total	0.862	0.138	1.000

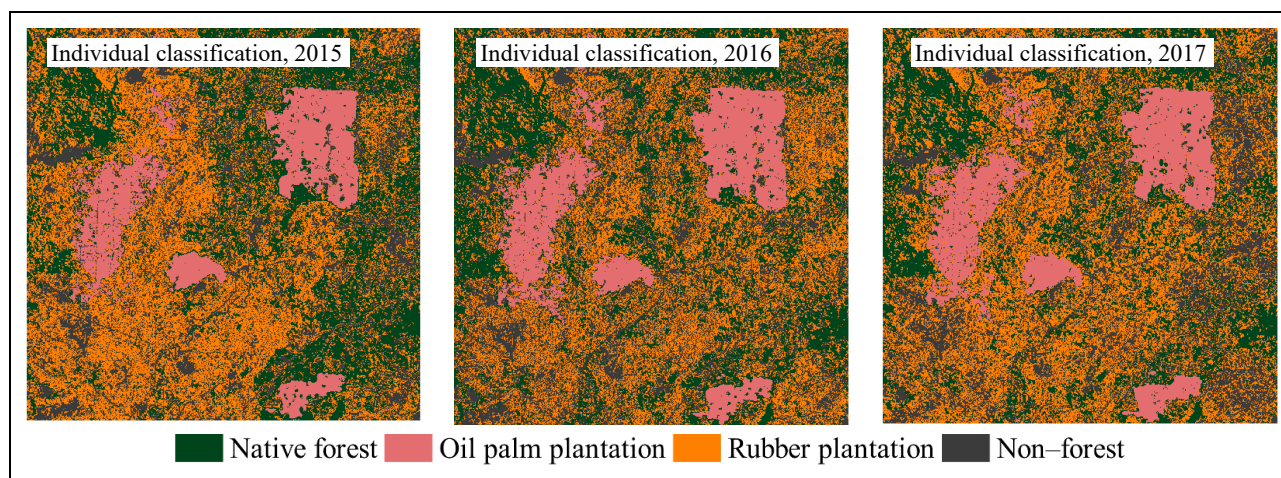
Table 3. Oil palm occurrence probability in 2016.

Time series class decision Land cover change 2016 to 2017	Probability similar to previous class	Probability to change class	Result of time series class for map in 2016
Native forest to Native forest	0.905	0.095	Native forest
Native forest to Oil palm	0.028	0.972	Oil palm
Native forest to Rubber	0.154	0.846	Rubber
Native forest to Non-forest	0.409	0.591	Non-forest
Oil palm to Oil palm	0.978	0.022	Oil palm
Oil palm to Rubber	0.530	0.470	Oil palm
Oil palm to Non-forest	0.994	0.006	Oil palm
Oil palm to Native forest	0.994	0.006	Oil palm
Rubber to Rubber	0.901	0.099	Rubber
Rubber to Non-forest	0.650	0.350	Rubber
Rubber to Native forest	0.848	0.152	Rubber
Rubber to Oil palm	0.001	0.999	Oil palm
Non-forest to Non-forest	0.871	0.129	Non-forest
Non-forest to Native forest	0.085	0.915	Native forest
Non-forest to Oil palm	0.027	0.973	Oil palm
Non-forest to Rubber	0.350	0.650	Rubber

Table 4. Decision-making result for time series classification for 2016 to 2017.

Images of individual year land cover classification, oil palm and rubber plantation occurrence, and the Bayesian network time series classification maps from 2015 to 2017 are shown in Figure 3.

Classification accuracy for the final time series land cover map in 2017 has an overall accuracy of 90%. Detailed accuracy for each land cover class is shown in Table 5.



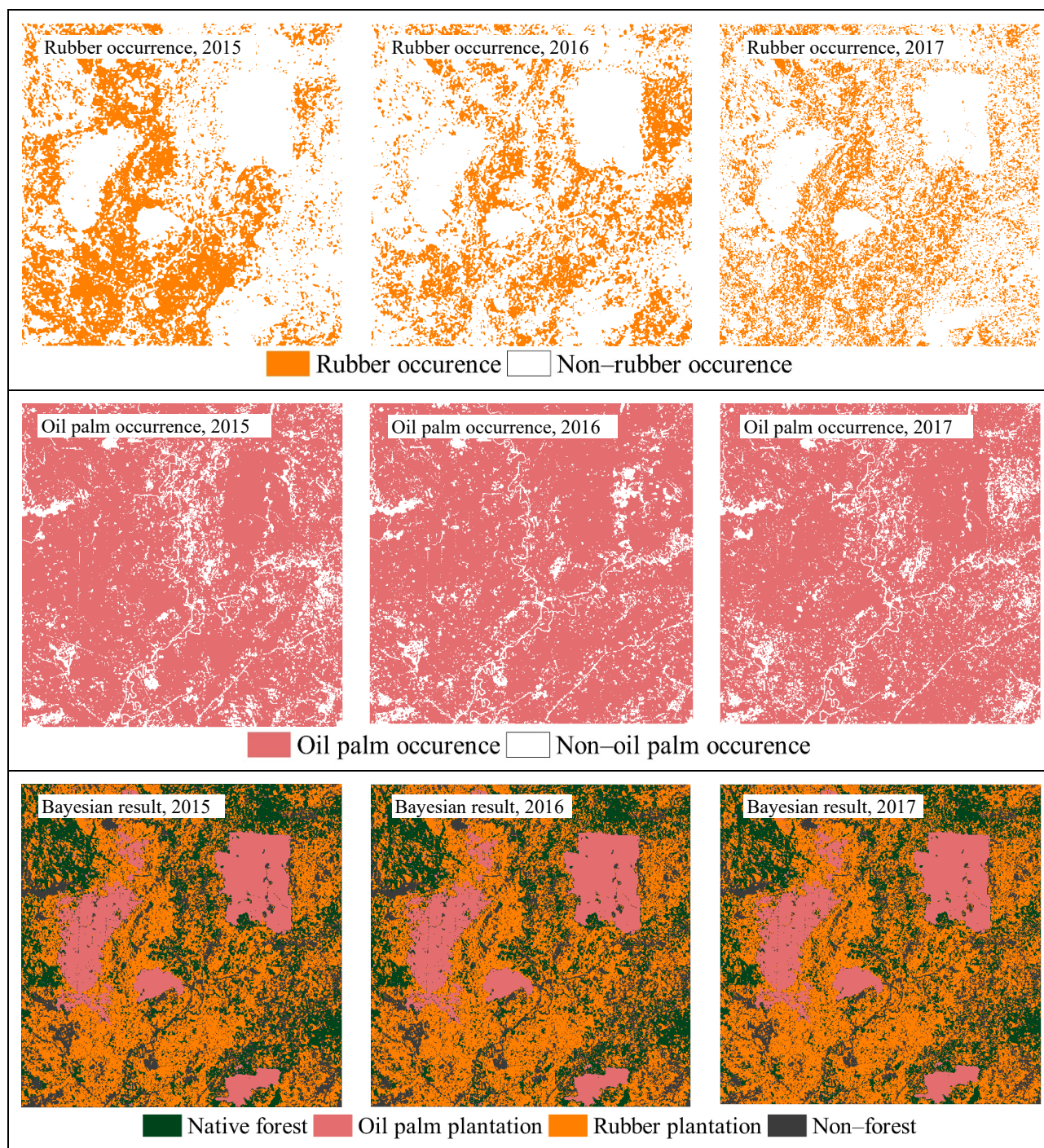


Figure 3. Individual year classification and time series classification images from 2015 to 2017

Reference data 2017 \ Classified data 2017	Reference data 2017				Total	User's acc. (%)
	Native forest	Oil palm	Rubber	Non-forest		
Native forest	38	0	3	0	41	93
Oil palm	2	25	0	0	27	93
Rubber	1	0	85	9	95	89
Non-forest	0	1	4	28	33	85
Total	41	26	92	37	196	
Producer's acc. (%)	93	96	92	76	Overall accuracy = 90%	

Table 5. Accuracy assessment of land cover classification in 2017.

Table 5 shows the Bayesian network time series classification map accuracy. User's and producer's accuracy for all land cover classes were >85%, which fulfils Indonesia's national land cover classification accuracy benchmark to support the national forest monitoring system (Badan Informasi Geospasial, 2014). Lower producer's accuracy for the non-forest class (76%) was primarily due to mixed classification between young rubber plantation and non-forest.

4. CONCLUSION

A Bayesian network algorithm was used to produce a time series of land cover classification that improved accuracy of individual year land cover maps for South Kalimantan, Indonesia. A time series of Landsat-8 optical and Sentinel-1 SAR images from 2015 to 2017 were used to develop temporal maps with four land cover classes: native forest, non-forests, rubber and oil palm plantations. High-resolution SPOT images were used for the accuracy assessment of the final 2017 map. The map generated using a Bayesian network produced overall accuracy of 90%. Moreover, each land cover class had a user's accuracy and producer's accuracy of >85%, except for the non-forest class which had producer's accuracy of 76% due to mixed classification between young rubber plantation and non-forest. The accurate time series land cover map that differentiates between native forests and non-forests and includes two additional plantation classes will support Indonesia's national forest monitoring system and development of sustainable forest management. These maps can help to predict future plantation development, and potentially protect forests thus reducing emissions from forest degradation and deforestation.

ACKNOWLEDGEMENTS

We thank the LCCA teams of LAPAN, the Indonesia–Australia Forest Carbon Partnership (IAFCP) for sharing data and methods. I.L.S acknowledges the Indonesian Endowment Fund for Education (LPDP) for PhD scholarship

REFERENCES

Badan Informasi Geospasial. Peraturan Kepala Badan Informasi Geospasial Nomor 15 Tahun 2014 Ten-Tang Pedoman Teknis Ketelitian Peta Dasar (Head of Geospatial Information Agency: Technical Guidelines to Determine the Accuracy of the Base Map Number 15 Year 2014); Geospatial Information Agency of Indonesia: Cibinong, Indonesia; 2014; p. 15. Available online: https://jdih.big.go.id/media/resources/files/law/tUF25Yj2xW_Perka_Ketelitian_Peta_Dasar_-_Salinan.pdf (accessed on 12 July 2021).

BPS Provinsi Kalimantan Selatan. Provinsi Kalimantan Selatan Dalam Angka 2000 (Kalimantan Selatan Province In Figures 2000); BPS-Statistics of Kalimantan Selatan Province: Banjarbaru, Indonesia, 2000.

BPS Provinsi Kalimantan Selatan. Provinsi Kalimantan Selatan Dalam Angka 2018 (Kalimantan Selatan Province In Figures 2018); BPS-Statistics of Kalimantan Selatan Province: Banjarbaru, Indonesia, 2018.

Ban, Y. Synergy of multitemporal ERS-1 SAR and Landsat TM data for classification of agricultural crops. *Canadian Journal of Remote Sensing* 2003, 29, 518-526, doi:<https://doi.org/10.5589/m03-014>.

Gaveau, D.L.A.; Locatelli, B.; Salim, M.A.; Yaen, H.; Pacheco, P.; Sheil, D. Rise and fall of forest loss and industrial plantations in Borneo (2000–2017). *Conserv. Lett.* 2018, 12, e12622. doi:<https://doi.org/10.1111/conl.12622>.

Hoekman, D.H.; Vissers, M.A.M.; Wieland, N. PALSAR wide-area mapping of Borneo: Methodology and map validation. *IEEE J. Sel. Top. Appl. Earth Observ. Remote. Sens.* 2010, 3, 605–617. doi:<https://doi.org/10.1109/JSTARS.2010.2070059>.

Hosonuma, N.; Herold, M.; De Sy, V.; De Fries, R.S.; Brockhaus, M.; Verchot, L.; Angelsen, A.; Romijn, E. An assessment of deforestation and forest degradation drivers in developing countries. *Environ. Res. Lett.* 2012, 7, 044009, doi:[doi:10.1088/1748-9326/7/4/044009](https://doi.org/10.1088/1748-9326/7/4/044009).

LAPAN. The Remote Sensing Monitoring Program of Indonesia's National Carbon Accounting System: Methodology and Products, Version 1; LAPAN-IAFCP: Jakarta, Indonesia, 2014; pp. 15–78. Available online:<http://incas.menlhk.go.id/methodology/incas-standard-method-forest-cover-change/> (accessed on 4 January 2019).

Lee, J.; Cardille, J.A.; Coe, M.T. Agricultural Expansion in Mato Grosso from 1986–2000: A Bayesian Time Series Approach to Tracking Past Land Cover Change. *Remote Sensing* 2020, 12, doi:<https://doi.org/10.3390/rs12040688>.

Massey, R.; Sankey, T.T.; Yadav, K.; Congalton, R.G.; Tilton, J.C. Integrating cloud-based workflows in continental-scale cropland extent classification. *Remote Sens. Environ.* 2018, 219, 162-179, doi:[doi:10.1016/j.rse.2018.10.013](https://doi.org/10.1016/j.rse.2018.10.013).

Miettinen, J.; Liew, S.C.; Kwoh, L.K. In Usability of Sentinel-1 dual polarization C-band data for plantation detection in insular Southeast Asia. In Proceedings of the 36th Asian Conference on Remote Sensing (ACRS2015), Quezon City, Metro Manila Philippines, 24–28 October 2015.

Motohka, T.; Shimada, M.; Uryu, Y.; Setiabudi, B. Using time series PALSAR gamma nought mosaics for automatic detection of tropical deforestation: A test study in Riau, Indonesia. *Remote Sens. Environ.* 2014, 155, 79-88, doi:[doi:10.1016/j.rse.2014.04.012](https://doi.org/10.1016/j.rse.2014.04.012).

Pohl, C. Mapping palm oil expansion using SAR to study the impact on the CO₂ cycle. In Proceedings of IOP Conference Series: Earth and Environmental Science; p. 012012.

Romijn, E.; Lantikan, C.B.; Herold, M.; Lindquist, E.; Ochieng, R.; Wijaya, A.; Murdiyarso, D.; Verchot, L. Assessing change in national forest monitoring capacities of 99 tropical countries. *Forest Ecology and Management* 2015, 352, 109-123, doi:[doi:10.1016/j.foreco.2015.06.003](https://doi.org/10.1016/j.foreco.2015.06.003).

Sari, I.L.; Weston, C.J.; Newnham, G.J.; Volkova, L. Assessing Accuracy of Land Cover Change Maps Derived from Automated Digital Processing and Visual Interpretation in Tropical Forests in Indonesia. *Remote Sensing* 2021a, 13, doi:[doi:10.3390/rs13081446](https://doi.org/10.3390/rs13081446).

Sari, I.L.; Weston, C.J.; Newnham, G.J.; Volkova, L. Estimating land cover map accuracy and area uncertainty using a confusion matrix: A case study in Kalimantan, Indonesia. *IOP Conference Series: Earth and Environmental Science* 2021b, 914, 012025, doi:[doi:10.1088/1755-1315/914/1/012025](https://doi.org/10.1088/1755-1315/914/1/012025).

Sari, I.L.; Weston, C.J.; Newnham, G.J.; Volkova, L. Developing Multi-Source Indices to Discriminate between Native Tropical Forests, Oil Palm and Rubber Plantations in Indonesia. *Remote Sensing* 2022, 14, doi:10.3390/rs14010003.

Sarzynski, T.; Giam, X.; Carrasco, L.; Lee, J.S. Combining Radar and Optical Imagery to Map Oil Palm Plantations in Sumatra, Indonesia, Using the Google Earth Engine. *Remote Sensing* 2020, 12, doi:<https://doi.org/10.3390/rs12071220>.

The Alaska Satellite Facility Distributed Active Archive Center (ASF DAAC). Sentinel-1. Available online:<https://www.asf.alaska.edu/>. (accessed on 3 July 2019).

The USGS Earth Resources Observation and Science (EROS) Center. Landsat. Available online: <https://earthexplorer.usgs.gov/>. (accessed on 3 July 2019).